Nuclear Instruments and Methods in Physics Research A 824 (2016) 721–725

Contents lists available at ScienceDirect

Nuclear Instruments and Methods in Physics Research A

journal homepage: www.elsevier.com/locate/nima

New results from the RD52 project

Richard Wigmans

Department of Physics, Texas Tech University, Lubbock, TX 79409-1051, USA

On behalf of the RD52 (DREAM) Collaboration

ARTICLE INFO

Available online 9 October 2015

Keywords:
Calorimetry
Dual-readout
Čherenkov light

ABSTRACT

Simultaneous detection of the Čerenkov light and scintillation light produced in hadron showers makes it possible to measure the electromagnetic shower fraction event by event and thus eliminate the detrimental effects of fluctuations in this fraction on the performance of calorimeters. In the RD52 (DREAM) project, the possibilities of this dual-readout calorimetry are investigated and optimized. In this talk, the latest results of this project will be presented. These results concern tests of a dual-readout fiber calorimeter with electrons at very small angles of incidence, detailed measurements of the time structure of hadron showers in this detector, as well as elaborate comparisons of various aspects of the calorimeter performance with GEANT4 simulations.

1. Introduction

The ideas that formed the basis for the RD52 project, as well as the detectors constructed by the DREAM Collaboration, were already presented at the previous Elba conference [1]. In our detectors, fluctuations in the electromagnetic shower component (f_{em}), which limit the performance of almost all calorimeters used in modern high-energy physics experiments, are eliminated by simultaneous measurements of the energy deposit dE/dx and the fraction of that energy carried by relativistic charged shower particles. We have experimentally demonstrated that this makes it possible to measure f_{em} event by event [2]. We use scintillation light and Čherenkov light as signals for the stated purposes. Therefore, this method has become known as the Dual REAdout Method (DREAM). It provides in practice the same advantages as intrinsically compensating calorimeters ($e/h = 1$), but are not subjected to the limitations of the latter devices: sampling fraction, signal integration time and volume, and especially the choice of absorber material. This has important consequences for the precision of jet measurements.

During most of the time since the previous conference, the CERN accelerator complex has been shut down because of LHC upgrade activities. We have used this period to carry out an extensive program of Monte Carlo simulations, both for electromagnetic and hadronic showers developing in our, in many ways, very unusual calorimeters. Many results of this work have been summarized in a recent paper [3]. At this conference, we report on results of new simulations with different hadronic shower packages. We also present new experimental data on the performance of our copper-fiber calorimeter for showers induced by electrons entering at very small angles with the fiber direction. These studies were inspired by GEANT4 predictions of unexpected phenomena. Finally, we also show very recent results on the time structure of the signals in our dual-readout lead-fiber calorimeter.

2. Hadronic performance

In our recent Monte Carlo paper, we showed that "standard" hadronic shower simulations gave a reasonable description of the response functions for 100 GeV π^- in the original DREAM copper-fiber calorimeter [3]. Especially the Čherenkov response function was well described by these simulations. On the other hand, the scintillation distribution was more narrow, less asymmetric and peaked at a lower value than for the experimental data. From additional analyses, we established that the non-relativistic component of the shower development, which is completely dominated by processes at the nuclear level, is rather poorly described by GEANT4, at least by the FTFP_BERT hadronic shower development package, which is the standard used by the ATLAS and CMS collaborations. Both the average size of this component, as well as its event-to-event fluctuations, are at variance with the experimental data. This non-relativistic shower component only plays a role for the scintillation signals, *not* for the Čherenkov ones.

Yet, some aspects of hadronic shower development that are important for the dual-readout application were found to be in good agreement with the experimental data, *e.g.*, the shape of the Čherenkov response function and the radial shower profiles.

E-mail address: wigmans@ttu.edu

http://dx.doi.org/10.1016/j.nima.2015.09.069
0168-9002/

Attempts to use the dual-readout technique on simulated shower data reasonably reproduced some of the essential characteristics and advantages of this method: a Gaussian response function, hadronic signal linearity and improved hadronic energy resolution. The fact that the reconstructed beam energy was systematically too low may be ascribed to the problems with the non-relativistic shower component mentioned above.

An important reason for performing these very time consuming simulations was to see if and to what extent the hadronic performance would improve as the detector size is increased. Fig. 1 (a) shows the signal distribution obtained for 100 GeV π^- in a copper based RD52 calorimeter with a lateral cross-section of 65×65 cm^2. The mass of such a (10 $\lambda_{\rm int}$ deep) device would be $\sim$ 6 tonnes. According to these simulations, which were carried out with the FTFP_BERT package, the average calorimeter signal, reconstructed with the dual-readout method, would be 90.2 GeV, and the energy resolution would be 4.6%.

In order to see to what extent these simulations depend on the choice of the hadronic shower development package, we repeated these simulations using the high precision version of the hadronic shower simulation package (FTFP_BERT_HP), which seems to provide a much more elaborate treatment of the numerous neutrons produced in the shower process, but also takes an order of magnitude more CPU time. Fig. 1(b) shows the results of this work. Indeed, the results show a clear improvement: the average calorimeter signal has increased to 95.6 GeV, and is thus within a few percent equal to that of an em shower developing in the same calorimeter structure (one of the crucial advantages of calorimeters based on the DREAM principle). Also the energy resolution improved significantly, from 4.6% to 3.2%. We also generated 4630 events for 200 GeV with the FTFP_BERT_HP package. This gave an average signal of 191 GeV and an energy resolution of 2.4%.

Fig. 2 summarizes the situation concerning the hadronic energy resolution, for single pions. Experimental data on hadronic performance compared to GEANT4 simulations are shown in Fig. 2(a). The experimental data obtained with the original DREAM fiber calorimeter, which had a lateral cross-section of 820 cm^2 [2], are compared with simulations using the standard FTFP_BERT hadronic simulation package for the geometry of that detector. The improvement expected for a larger detector (65×65 cm^2 lateral cross-section) with the RD52 geometry is also shown, both for the standard FTFP_BERT package and for the high-precision version of this package. For comparison, the record setting experimental data reported by SPACAL [4] are also shown, as well as a curve representing an energy resolution of $30\%/\sqrt{E}$.

We believe that the predicted improvement in the performance resulting from an increased detector size is realistic. The resolution of the instruments tested so far was clearly dominated by leakage fluctuations. An increase in the detector volume would reduce the effects of this, in which case resolutions of a few percent seem to be feasible, and would bring the hadronic performance of the RD52 calorimeter at the same level as that of the compensating SPACAL and ZEUS calorimeters, or even better. The potential importance of this is illustrated in Fig. 2(b), which shows the results of the simulation of a mixture of hadron showers with energies corresponding to the masses of the W and Z bosons. The two peaks are clearly separated, which is a design requirement for calorimeters at future e^+e^- colliders. Of course, just like with all other hadron calorimeter results, these simulations need to be verified experimentally in order to establish how realistic they really are.

It should be emphasized that the results shown in Figs. 1 and 2 are for *single hadrons*. There is an important reason why the jet energy resolution of copper based dual-readout fiber calorimeters may also be expected to be much better than that of the high-Z compensating calorimeters [1]. A sizable component of the jet consists of soft hadrons, which range out rather than developing showers. The response of calorimeters such as ZEUS to these particles was considerably larger than the response to the showering γs and high-energy hadrons. The scale for the difference between these responses is set by the e/mip value, which was measured to be 0.62 in ZEUS [5] and 0.72 in SPACAL [6]. The advantage of an absorber material with much lower Z is an e/mip value that is much closer to 1 (the value at which point this effect ceases to play a role). For our copper based dual-readout fiber calorimeter, an e/mip value of 0.84 was found [7]. The possibility to measure jets with superior resolution compared to previously built high-Z compensating calorimeters was one of the main reasons why we embarked on the dual-readout project.

3. Electromagnetic performance

After a long shutdown, the SPS became again available for testbeam work at the end of 2014. We used the allocated beam time to carry out a study of the performance of our RD52 copper-fiber calorimeter for 20 GeV electrons entering the detector at very small angles of incidence, i.e. almost parallel to the fiber direction. This study was inspired by the fact that our

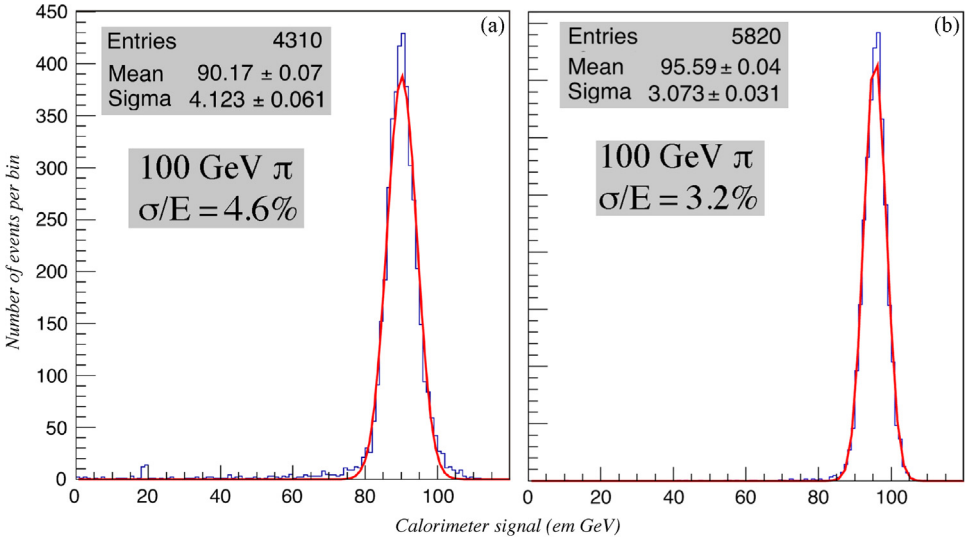

Fig. 1. GEANT4 simulations of the response function to 100 GeV π^- particles of a dual-readout fiber calorimeter with the RD52 structure, and lateral dimensions of 65×65 cm^2. Results are shown for the standard FTFP_BERT hadronic shower simulation package (*a*), and with the high-precision version of this package, FTFP_BERT_HP (*b*).

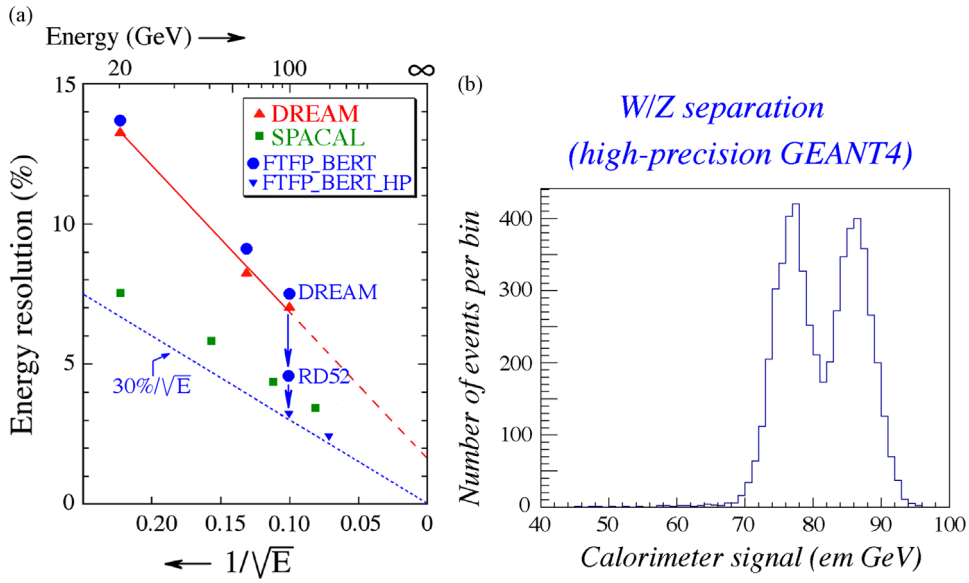

Fig. 2. Experimental data on hadronic performance compared to GEANT4 simulations (*a*). See text for details. Diagram *b* shows the results of a simulation for a mixture of hadrons with the energies of the *W* and *Z* vector bosons, using the high-precision hadronic shower simulation package.

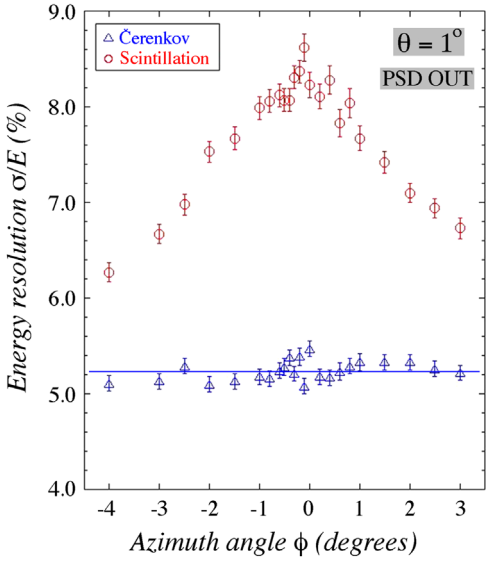

Fig. 3. The energy resolution measured for 20 GeV electrons in the scintillation and the Čherenkov channels, as a function of the azimuth angle of incidence (ϕ) of the beam particles. The tilt angle θ was 1°.

Monte Carlo simulations predicted some very specific effects [3]. We have recently submitted a paper containing many results of this study [8]. Here, we only discuss one of these results, namely the difference in the angular effects on the energy resolution for the two types of signals (Fig. 3). Not only is the energy resolution significantly worse for the scintillation signals, for all angles in this range, but the resolution measured for the scintillation signals also depends strongly on the angle of incidence, unlike the resolution measured with the Čherenkov signals.

These results are consistent with earlier observations that the energy resolution at a fixed angle of incidence ($\phi = 1.5°, \theta = 1.0°$) tends to become better for the Čherenkov signals than for the scintillation ones as the energy of the electron beam increases [9]. Since the sampling structure is the same for both types of fibers, and the light yield considerably larger (and event-to-event fluctuations in the number of scintillation photoelectrons thus correspondingly smaller), one would naively expect to measure better energy resolutions for the scintillation signals. The fact that the opposite effect is experimentally observed is a consequence of the extremely collimated nature of the em showers in the early stage of the shower development, before the shower maximum is reached, i.e. in the first 10 cm of this particular calorimeter.

Neighboring fibers *of the same type* are separated by 2–3 mm and that distance is of the same order as the shower width in this early stage of the shower development. Therefore, the calorimeter signal (from this early shower component) depends crucially on the impact point of the particles, if these enter the calorimeter parallel to the fibers. This dependence is quickly reduced when the particles enter the calorimeter at a small angle with the fibers. As the angle increases, this early collimated shower component is thus sampled more and more in the same way as the rest of the shower. However, at angles where this is not the case, this effect adds an additional component to the em energy resolution. This effect is, in first approximation energy independent and thus acts as a constant term.

Now, why does this only affect the resolution measured with the scintillation signals? The reason is that the collimated early shower component does *not* contribute to the Čherenkov signals, since the Čherenkov light produced by shower particles traveling in the same direction as the fibers falls outside the numerical aperture of the fibers. For the 20 GeV electrons, the Čherenkov fibers thus only register shower particles that travel at relatively large angles with the shower axis (20–60°), and such particles are for all practical purposes only found beyond the shower maximum, where the shower is wide compared to the typical distance separating neighboring fibers of the same type. The "constant" term that affects the scintillation resolution is thus practically absent for the Čherenkov signals.

The Čherenkov resolution is completely determined by sampling fluctuations and by fluctuations in photoelectron statistics, both of which are independent of the angle of incidence in these measurements, and both of which contribute about equally to the measured resolution. Since the scintillation light yield is more than an order of magnitude larger than the Čherenkov one, the contributions of the (angle independent) fluctuations in photoelectron statistics are negligible for the energy resolution measured with the scintillation signals.

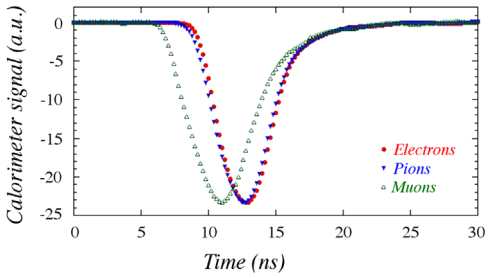

Fig. 4. Average time structure of the Čherenkov signals produced by the RD52 lead-fiber calorimeter, for 40 GeV electrons, pions and muons. The time base was started by the signal in the upstream trigger counters.

4. Time structure of the showers

A second part of our measurements in 2014 concerned the time structure of the signals provided by our dual-readout fiber calorimeters. We used the 36-tower lead-fiber calorimeter for this purpose. This calorimeter was surrounded by a set of 20 leakage counters, blocks of plastic scintillator with dimensions $50 \times 50 \times 10$ cm^3. In total, 30 different signals were read out with a CAEN V1742 switched capacitor digitizer, based on the DRS4 chip [10]. This device provided 5 Gs/s digitization of these signals.

A crucial aspect of the RD52 fiber calorimeter is its *longitudinally unsegmented* structure. The detailed time structure of each event makes it possible to obtain crucial information about the depth at which the light is produced. By using the fact that light travels at a speed of c/n in the fibers, while the particles producing the light travel in general at velocities close to c, the starting time of the signals makes it possible to measure the depth at which the light is produced with a resolution of ~ 20 cm [1]. This allows us to correct for small effects of light attenuation in the fibers and is an important tool for electron/photon identification [11]. The time structure also turns out to be an important tool for measuring the neutron contribution to the scintillation signals [12].

The results shown here concern a 40 GeV positive beam, which consisted of a mixture of electrons, pions and muons. The different particles were identified with external counters, i.e. the preshower detector, a tail catcher and the muon counter. The following plots show the average time structures for a few thousand particles of each type. In order to appreciate these figures, one should realize that the deeper the light was produced inside the calorimeter, the earlier the resulting signal was recorded. The size of this effect amounted to ~ 2.5 ns/m.

Fig. 4 shows the average time structure of the Čherenkov signals from the calorimeter tower into which the beam particles were steered. The muons produced light over the full 2.5 m length of the calorimeter module, and therefore the signals started earlier than for the electrons and pions, which produced most of the light close to the front face of the calorimeter. The shower maximum for the pions was located about 20 cm deeper inside the calorimeter than for electrons, and therefore the pion signals also started a bit earlier than the electron ones.

The scintillation signals for the same events had a longer duration. This is due to the time constant that is characteristic for the scintillation process, plus the fact that the non-relativistic particles which contributed to the scintillation signals (but not to the Čherenkov ones) were distributed over a greater depth in the calorimeter volume than the relativistic ones.

The pion component of the beam was also completely responsible for any signals recorded by the leakage counters. Fig. 5 (a) shows the average signals recorded in two different leakage counters. These counters were located close to the shower maximum (the early signal), and near the end of the calorimeter module (the late signal). The latter signal consisted very likely

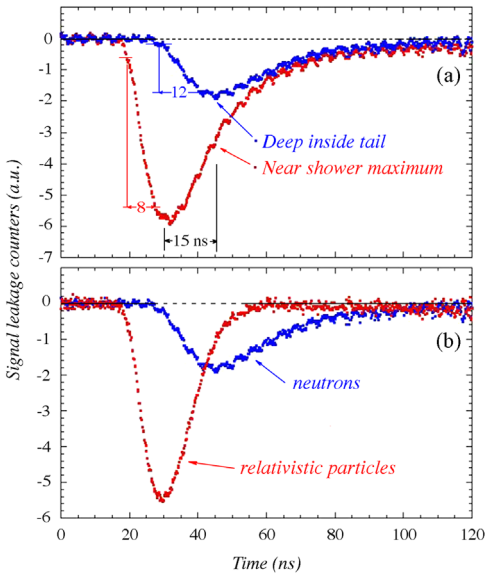

Fig. 5. Average time structure of the signals measured in leakage counters surrounding the RD52 lead-fiber calorimeter, for 40 GeV π^- steered into the center of this calorimeter. Diagram *a* shows the signals measured in a counter located close to the shower maximum (not far from the front face of the calorimeter) and in a counter located near the shower tail, i.e. about 2 m from the front face of the calorimeter. In diagram *b*, the signal from the upstream counter is unfolded into a "neutron" and a "prompt" component. See text for details.

exclusively of recoil protons produced by elastic neutron scattering, while the early signal may also contain a contribution from relativistic particles produced in the shower development and escaping the calorimeter. In the hadronic shower development, typically a few thousand neutrons are released from the nuclei in which they were bound. They typically carry a few MeV kinetic energy and lose that energy predominantly by means of elastic scattering off protons in the plastic components of the detectors, with a time constant of ~ 10 ns [13].

In Fig. 5(b), the average signal from the leakage counter located near the shower maximum is unfolded into a "prompt" and a "neutron" component, by assuming that the latter component is completely responsible for the trailing edge of the signals. The figure shows that the time difference between the two signal components obtained in this way, as well as the difference between the rise times of these two signal components, are consistent with the assessment that the signals from this leakage counter were caused by a mixture of slow neutrons and relativistic shower particles. We expect to be able to extract much more information out of these data than shown here. We are also planning follow-up measurements with a much faster light detector.

References

[1] R. Wigmans, Nuclear Instruments and Methods in Physics Research Section A 718 (2013) 43.
[2] N. Akchurin, et al., Nuclear Instruments and Methods in Physics Research Section A 537 (2005) 537.
[3] N. Akchurin, et al., Nuclear Instruments and Methods in Physics Research Section A 762 (2014) 100.
[4] D. Acosta, et al., Nuclear Instruments and Methods in Physics Research Section A 308 (1991) 481.
[5] G. Drew, et al., Nuclear Instruments and Methods in Physics Research Section A 290 (1990) 335.
[6] D. Acosta, et al., Nuclear Instruments and Methods in Physics Research Section A 320 (1992) 128.
[7] N. Akchurin, et al., Nuclear Instruments and Methods in Physics Research Section A 533 (2004) 305.

[8] A. Cardini, et al., Nuclear Instruments and Methods in Physics Research Section A 15 (2015).
[9] N. Akchurin, et al., Nuclear Instruments and Methods in Physics Research Section A 735 (2014) 130.
[10] S. Ritt, et al., Nuclear Instruments and Methods in Physics Research Section A 623 (2010) 486.
[11] N. Akchurin, et al., Nuclear Instruments and Methods in Physics Research Section A 735 (2014) 120.
[12] R. Wigmans, Nuclear Instruments and Methods in Physics Research Section A 617 (2010) 129.
[13] R. Wigmans, Calorimetry, Energy Measurement in Particle Physics, International Series of Monographs on Physics, 107, Oxford University Press, Oxford, United Kingdom, 2000.